Biodegradable electroactive polymers for electrochemically-triggered drug delivery

DOI: 10.1039/C4TB00355A (Paper) J. Mater. Chem. B, 2014, **2**, 6809-6822

Biodegradable electroactive polymers for electrochemically-triggered drug delivery†

John G. Hardy *[ab], David J. Mouser [a], Netzahualcóyotl Arroyo-Currás [c], Sydney Geissler [ab], Jacqueline K. Chow [a], Lindsey Nguy [a], Jong M. Kim [a] and Christine E. Schmidt *[ab]
[a]Department of Biomedical Engineering, The University of Texas at Austin, Austin, TX 78712, USA. E-mail: johnhardyuk@gmail.com
[b]J. Crayton Pruitt Family Department of Biomedical Engineering, University of Florida, Biomedical Sciences Building JG-53, P.O. Box 116131, Gainesville, FL 32611-6131, USA. E-mail: schmidt@bme.ufl.edu
[c]Center for Electrochemistry, Chemistry Department, The University of Texas at Austin, Austin, TX 78712, USA

Received 2nd March 2014 , Accepted 19th August 2014

First published on the web 19th August 2014

We report biodegradable electroactive polymer (EAP)-based materials and their application as drug delivery devices. Copolymers composed of oligoaniline-based electroactive blocks linked to either polyethylene glycol or polycaprolactone blocks via ester bonds were synthesized in three steps from commercially available starting materials and isolated without the need for column chromatography. The physicochemical and electrochemical properties of the polymers were characterized with a variety of techniques. The ability of the polymers to deliver the anti-inflammatory drug dexamethasone phosphate on the application of electrochemical stimuli was studied spectroscopically. Films of the polymers were shown to be degradable and cell adhesive in vitro. Such EAP-based materials have prospects for integration in implantable fully biodegradable/bioerodible EAP-based drug delivery devices that are capable of controlling the chronopharmacology of drugs for future clinical application.

Introduction

Systems capable of precisely controlling levels of drugs in specific tissues or the blood stream potentially allow maintenance of the drug above its minimum effective level and below the level at which its use results in unwanted side effects. Furthermore, as our understanding of chronobiology has deepened, we have become aware of its importance in a variety of conditions including Alzheimer's disease, cancer, cardiovascular diseases, diabetes, epilepsy, pain, Parkinson's disease and infectious diseases.[1–3] Such conditions can be treated most effectively by drugs with chronopharmacologies synchronized with the chronobiology of the specific condition.[2–6] Chronobiological processes that are governed on a genetic level by clock genes display rhythmic endogenous oscillations driven by the circadian clock (i.e.

circadian rhythms). Perturbations of circadian rhythms are involved with a variety of conditions (including cancers, depression, diabetes, and sleep disorders), as discussed in detail in a selection of excellent reviews,[1,7–11] and such conditions are attractive targets for chrono-specific treatments.[12–14]

Stimuli-responsive drug delivery systems are particularly attractive for the treatment of such conditions because of their potential for the controlled delivery of precise quantities of drugs at specific locations and times. Materials responding to stimuli such as enzymes, light, pH, temperature, ultrasound and electric/magnetic fields have been developed for use as drug delivery devices.[2,3,6,15–30] An exciting new research area is the development of electroactive materials capable of controlling either cell behavior or the delivery of drugs.[31–35] Here we report the first application of biodegradable EAP-based materials for electrochemically-triggered drug delivery.

EAPs are of scientific interest because of their potential for application in the electronics[36–38] and biomedical[31–33,35,39–59] industries. Although there are a number of different EAPs,[36–39,56,60,61] those most commonly investigated for biomedical applications are derivatives of polyaniline, polypyrrole, polythiophene and poly(3,4-ethylenedioxythiophene).[31–33,50,56,57,62] The highly conjugated backbone of EAPs synthesized via conventional means (e.g., electrochemical polymerization of the constituent monomers at the surface of an electrode, or the solution/solid state polymerization of the monomers in the presence of a catalyst) is responsible for their high conductivity, and the lack of enzymatically cleavable moieties (e.g., amides or esters) renders them non-biodegradable. Clearly, non-biodegradable EAPs are best suited for devices that will be implanted for long periods such as electrodes for the recording or stimulation of neuronal activity,[51,52] whereas, biodegradable EAPs are ideal for devices implanted for comparatively short durations such as drug delivery devices or tissue scaffolds.[33,35,63–67] The Miller group reported the first conceptually biodegradable EAPs in 1995.[68] The multiblock copolymers were composed of electroactive oligothiophenes and non-electroactive aliphatic spacers connected via ester bonds; however, iodine (a toxic oxidizing agent) was necessary to render them electroactive.[68] Analogous structures described in the literature incorporated electroactive oligomers that were insoluble or aggregated in water.[69] This approach is not ideal for clinical applications as the insoluble/aggregated oligomers are likely to remain in the body after degradation of the bulk material. Rivers and co-workers were the first to report the preparation of fully biodegradable electroactive polyesters incorporating a water soluble electroactive oligomer (pyrrole–thiophene–pyrrole) displaying carboxylic acids at their termini,[70] however, similar to earlier work, these polymers were only electroactive after oxidation with iodine. Guimard and co-workers subsequently described analogous systems in which the length of the electroactive oligomer was increased from 3 to 4 heterocycles that could be doped with biocompatible anions (either chloride, Cl^-, or perchlorate, ClO_4^-) and the resulting polymers were suitable for the attachment and proliferation of Schwann cells in vitro.[71] The groups of Albertsson and Wei have reported a variety of biodegradable electrically EAPs through various combinations of short water soluble oligomers of aniline and biodegradable polymers of natural or synthetic origins.[35,72–84] Electrical stimulation of cells attached to the surfaces of camphorsulfonic acid-doped (CSA, Fig. 1) materials was demonstrated to enhance neurite extension from rat neuronal pheochromocytoma (PC12) cells,[84] and increase levels of early markers of osteogenic differentiation of preosteoblastic MC3T3-E1 cells.[85] Researchers have begun to address the cytotoxic degradation products of these polymers seen in vitro,[86–88]via the synthesis of oligoaniline analogues with reduced toxicities.[86,87] The interested reader is directed towards

the following recent reviews for a more thorough discussion of the potential of such materials for biomedical applications.[32,33,35,50,51,55,56]

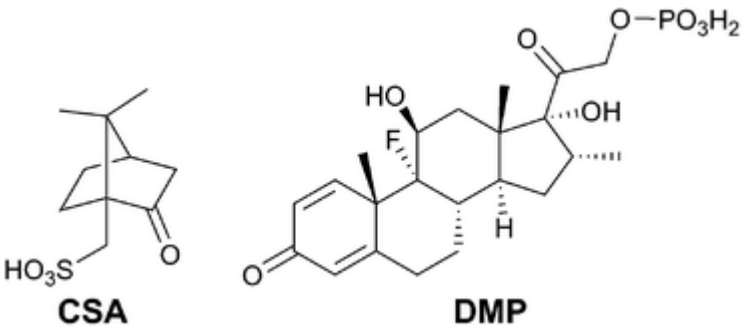

Fig. 1 Camphorsulfonic acid (CSA) and dexamethasone phosphate (DMP).

The Miller group was also the first to report the application of EAPs for drug delivery, demonstrating the ability to trigger the release of glutamate anions from polypyrrole films upon reduction of the polypyrrole.[89] Since this exciting report, a variety of other biologically relevant anionic, cationic and neutral drugs with either low/high molecular weights have been shown to be deliverable using EAP-based materials (e.g., adenosine triphosphate,[90] dexamethasone phosphate (DMP, Fig. 1),[91–93] DNA,[94] dopamine,[95,96] nerve growth factor,[97]N-methylphenothiazine[98]), as described in more detail in excellent reviews.[55,58] It is noteworthy that all of the previously described systems use non-biodegradable EAPs as the stimulus-responsive matrix from which to deliver the drug. Here we report the first biodegradable EAP-based drug delivery devices, employing solution-processable EAPs that facilitate the preparation of materials with high drug loadings (16 to 31 wt%).

Results and discussion

Our prototypical biodegradable electroactive polyesters are multiblock copolymers composed of electrochemically responsive blocks of oligoaniline terminated with carboxylic acid moieties to ensure their water solubility, linked to alcohol-terminated blocks of either FDA-approved polyethylene glycol (PEG) or polycaprolactone (PCL) via ester bonds. The molecular weight of each of the individual blocks is below 3 kDa, well below the renal filtration threshold of 70 kDa.[99–101]

The carboxylic acid-terminated aniline pentamers (AP) were obtained in analytically pure form using minor modifications to the methodology described in the literature (Scheme S1†).[102] Polyesters **1–4** were synthesized by adaptation of the literature.[81] In short, the carboxylic acids displayed at the termini of the electroactive AP blocks were activated with dicyclohexylcarbodiimide (DCC) in the presence of a catalytic amount of 4-dimethylaminopyridine (DMAP) and a stoichiometric quantity of alcohol-terminated PEGs (Scheme 1) or PCLs (Scheme 2), incorporating PEG-400, PEG-2000, PCL-530 or PCL-2000 to prepare polyesters **1**, **2**, **3** or **4** respectively. The syntheses and purifications of the polyesters are simple and scalable, requiring only three steps from commercially available starting materials and no column chromatography. The success of the condensation polymerization was confirmed by the presence of the characteristic peaks for esters in the IR spectra (at ca. 1732 cm^{-1}) and ^{13}C NMR spectra (at ca. 174 ppm), and thermogravimetric analysis (TGA) confirmed that the diacid and diol blocks were present in a 1 : 1 ratio (Fig. S1

and Table S1†). However, poor solubility (Table S2†) meant that determination of the molecular weight distributions of polyesters **1–4**via standard techniques such as GPC/SEC, light scattering or MALDI-TOF mass spectrometry was not possible.

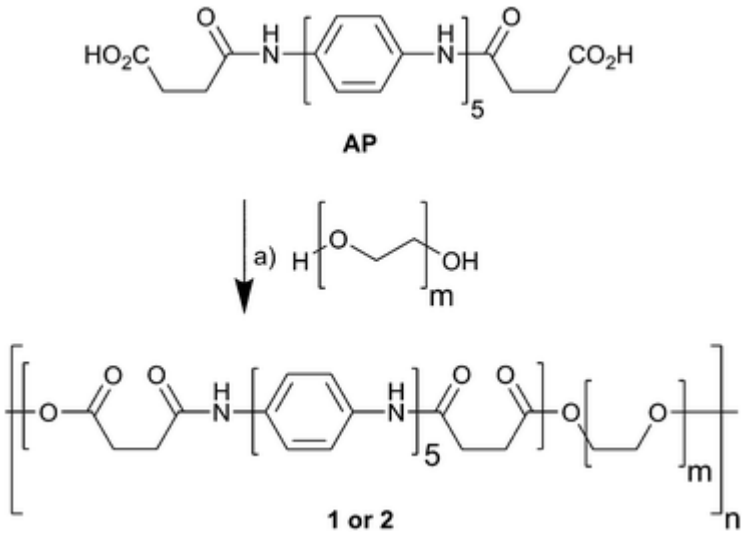

Scheme 1 Synthesis of electroactive polyesters **1** and **2**via the Steglich esterification. (a) DCC, DMAP, NMP, 72 h, r.t.

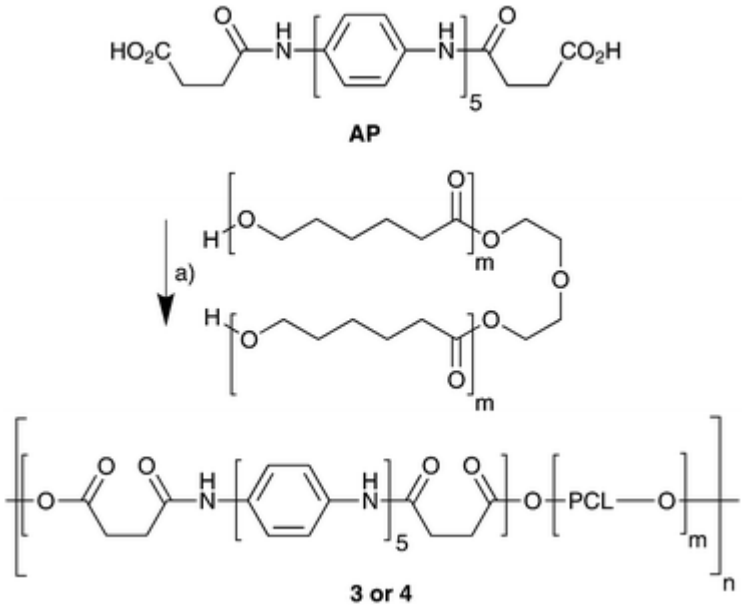

Scheme 2 Synthesis of electroactive polyesters **3** and **4**via the Steglich esterification. (a) DCC, DMAP, NMP, 72 h, r.t.

We prepared CSA-doped films of the polyesters to compare their physicochemical properties with analogous oligoaniline-based materials reported in the literature. Black films of ca. 20 μm thickness (as determined by profilometry) were prepared by casting solutions of the polymers and CSA in hexafluoroisopropanol (HFIP). Vacuum dried films of polyesters **1**, **3** and **4** were glossy, whereas those of polyester **2** were matte with spherulites owing to the crystallization of the PEG blocks. The wide angle XRD patterns for the films composed of polyesters **1**, **3** and **4** are very broad, characteristic of polymers that are amorphous in the

solid state (Fig. S2†). The wide angle XRD patterns for the films composed of polyester **2** contain peaks at 2θ = 19.1° and 23.3°, corresponding to d-spacings of 4.6 Å and 3.8 Å respectively, which are characteristic of crystalline PEG chains (Fig. S2† and Table 1).[103] In agreement with the literature, doping with bulky CSA anions reduced the crystallinity (X_c) of films of polyester **2** (Table 1).[104] CSA doping also diminished the thermal stability of the films, as revealed by TGA (Fig. S1†) and reductions in glass transition temperatures (T_g) of polyesters **1**, **3** and **4**, and the melting and crystallization temperatures (T_m and T_c respectively) of polyester **2** as measured by differential scanning calorimetry (DSC) (Fig. S3† and Table 1). IR spectra of the CSA-doped films (Fig. S4†) show peaks characteristic of electroactive AP blocks, either the PEG or PCL blocks respectively, and the esters interspersed between them. UV-visible spectra of thin films of the polymers cast on quartz slides (Fig. 2) show peaks at ca. 330 nm corresponding to the benzenoid π–π* transition in the AP blocks and are evident for all samples; the peaks at ca. 442 nm evident in the CSA-doped films correspond to the polaron band; the broad absorption after ca. 866 nm confirms the presence of emeraldine salts of the AP blocks, and the broad absorption after ca. 1000 nm corresponds to the "free carrier tail" reported for analogous electroactive block copolymers.[88,105]

Table 1 Surface and physicochemical properties of the polyester films

	R_a (μm)	**R_q (μm)**	**R_zDIN (μm)**	**X_c**	**T_g (°C)**	**T_c (°C)**	**T_m (°C)**	**Conductivity, σ (S cm^{-1})**
a As determined by XRD. b Not applicable. c Amorphous. d Not determined (below 0 °C).								
Glass substrate	0.730 ± 0.153	0.905 ± 0.182	3.8303 ± 2.04	N/A[b]	N/A[b]	N/A[b]	N/A[b]	N/A[b]
Polyester **1** undoped	1.474 ± 1.449	4.312 ± 3.684	12.099 ± 11.493	0.0	72.4	N/A[b,c]	N/A[b,c]	1.81×10^{-9} ± 6%
Polyester **1** doped with CSA	0.461 ± 0.421	0.530 ± 0.485	1.109 ± 0.710	0.0	51.5	N/A[b,c]	N/A[b,c]	3.38×10^{-8} ± 1%
Polyester **2** undoped	11.49 ± 1.26	12.926 ± 1.089	44.196 ± 3.155	49.8	N/D[d]	22.7	53.1	4.01×10^{-10} ± 14%
Polyester **2** doped with CSA	0.449 ± 0.061	0.572 ± 0.099	2.717 ± 0.523	13.4	N/D[d]	28.4	53.4	8.34×10^{-8} ± 2%
Polyester **3** undoped	0.303 ± 0.051	0.479 ± 0.182	1.669 ± 0.535	0.0	50.5	N/A[b,c]	N/A[b,c]	1.80×10^{-9} ± 6%
Polyester **3** doped with CSA	0.668 ± 0.082	1.111 ± 0.178	2.649 ± 0.874	0.0	37.6	N/A[b,c]	N/A[b,c]	6.14×10^{-9} ± 3%
Polyester **4** undoped	0.273 ± 0.191	0.315 ± 0.218	0.747 ± 0.542	0.0	41.8	N/A[b,c]	N/A[b,c]	6.04×10^{-10} ± 14%
Polyester **4** doped with CSA	0.598 ± 0.097	0.727 ± 0.147	1.674 ± 0.173	0.0	39.7	N/A[b,c]	N/A[b,c]	2.20×10^{-8} ± 2%

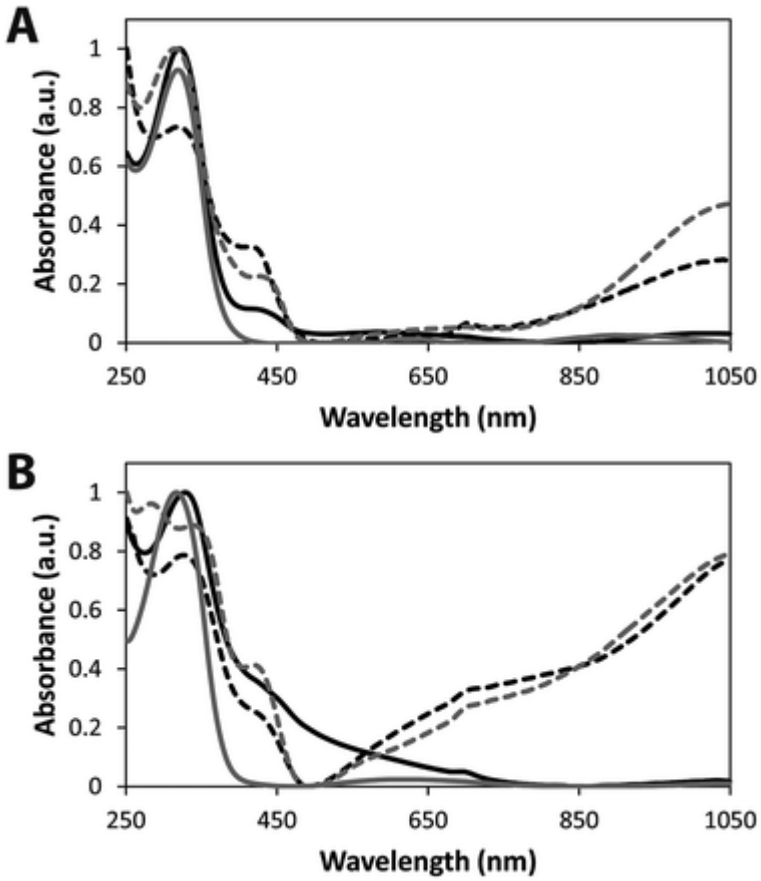

Fig. 2 UV-visible spectra of thin polyester films on quartz slides. (A) Polyester **1** undoped, black line; polyester **1** doped with CSA, dashed black line; polyester **2** undoped, grey line; polyester **2** doped with CSA, dashed grey line; (B) polyester **3** undoped, black line; polyester **3** doped with CSA, dashed black line; polyester **4** undoped, grey line; polyester **4** doped with CSA, dashed grey line.

Cyclic voltammograms of HCl-doped solutions of polyesters **1–4** (Fig. S5†), presented redox processes at ca. 0.26 V (leucoemeraldine to emeraldine 1 transition), ca. 0.42 V (emeraldine 1 to emeraldine 2 transition), and ca. 0.6 V (emeraldine 2 to pernigraniline transition), in agreement with the literature[76,78] and depicted in Scheme S2.† Potentials are reported vs. a Ag/AgCl reference electrode calibrated with ferrocenemethanol prior to every experiment (Fig. S6†).

The conductance of films of polyesters **1–4** were measured in accordance with protocol IPC-TM-650, number 2.5.17.2 of the Institute for Interconnecting and Packaging Electronic Circuits. Undoped polyesters had low conductivities on the order of 10^{-10} or 10^{-9} S cm^{-1}. Doping with CSA moderately higher conductivities, typically by an order of magnitude to 10^{-9} or 10^{-8} S cm^{-1} (Table 1), that are somewhat lower than analogous oligoaniline-based structures.[35,72,75,77,78,88] Polyesters incorporating the low molecular weight diols (polyesters **1** and **3**) had lower conductivities than the polyesters incorporating higher molecular weight diols (polyesters **2** and **4**), probably because the higher molecular weight diols in polyesters **2** and **4** phase separate into PEG- or PCL-rich phases and AP-rich phases. Other researchers have concentrated on developing biodegradable/bioerodible tissue scaffolds with conductivities mimicking bodily tissues (typically in the range of 10^{-4} S cm^{-1} or higher)[106–108]

to deliver biomimetic electric currents (in the μA regime) to electrically stimulate cells.[109–114] However, for our envisioned application as implantable devices for electrochemically-triggered drug delivery, conductivities lower than mammalian tissues are preferable, and allow triggered drug release at specific points in time upon the application of an electrical potential directly to the EAP, thereby facilitating synchronized control of the chronopharmacology of the drug in line with the chronobiology of the specific condition.

We studied the capability of the oligoaniline-based polymers to deliver an anti-inflammatory drug dexamethasone phosphate (DMP, MW 490 Da) into phosphate buffered saline (PBS). Dexamethasone was chosen because it is used in the clinic (often in multiple doses) and it is simple to monitor its release via UV spectroscopy. Films composed of polyesters **1–4** and DMP (of ca. 3 to 4 mg) were prepared on bioinert conductive and non-conductive substrates (glassy carbon electrodes and glass, respectively). DMP loadings were at a mole ratio of 1 : 1 DMP : AP (ca. 31 wt% for polyesters **1** and **3**, and ca. 16 wt% for polyesters **2** and **4**). The experimental setups are depicted in Fig. S7.† The setup depicted in Fig. S7A† (using films deposited on glassy carbon substrates) is akin to that used for electrodes implanted for stimulation of the central nervous system in which the tissue surrounding the implant is used as a counter electrode.[51,52,59,115,116] The setup depicted in Fig. S7B† (using films deposited on glass substrates) is a simple closed circuit similar to those proposed to power some electroactive tissue scaffolds.[32–34]

Electrochemically-triggered release (i.e., de-doping) of DMP from the films was studied by voltammetry for films deposited on glassy carbon substrates. Evidence of the electrochemical de-doping process was clear from the sequentially diminished current densities during repetitive potential cycling of the films at v = 50 mV s^{-1} (Fig. S8–S11† for polyesters **1–4**), concomitant with increasing absorbance of the PBS at the characteristic absorbance maximum of DMP (242 nm) as observed via UV spectroscopy. Pulsatile release from films deposited on glassy carbon substrates was studied by chronoamperometry using 1 minute of electrical stimulation followed by 14 minutes of rest (Fig. 3A) after which the quantity of DMP in solution was quantified by UV spectroscopy. The medium was unchanged between cycles. The data are reported as cumulative release as a percentage of the total mass of drug in the film and compared to DMP release from unstimulated films. Voltammetry scans and chronoamperometry pulses were always initiated at the open circuit potential of the system. Potential cycling was carried out between 0.7 V and −0.5 V, first sweeping in the positive direction of the potential scale at 50 mV s^{-1}. Passive release of DMP from unstimulated films was low over the course of the experiment (1.5 hours), ca. 8% for polyester **1**, ca. 3% for polyester **2** and ca. 2% for polyesters **3** and **4** (Fig. 3B). Over the period of 24 days this increased to ca. 83% for polyesters **1** and **2**, ca. 48% for polyester **3** and ca. 35% for polyester **4** (Fig. S12†). Passive release from the PEG-based polyester films (i.e. polyesters **1** and **2**) was higher than from the PCL-based polyester films (i.e. polyesters **3** and **4**) due to the more hydrophilic nature of the PEG backbones. In contrast, electrochemically-triggered release of the drugs by potential cycling (Fig. 3B) resulted in the release of ca. 20–65% of the drug during the initial cycle. Subsequent cycles were observed to release 5–10% per cycle for the first six cycles, after which the majority of the drug had been released from all of the films.

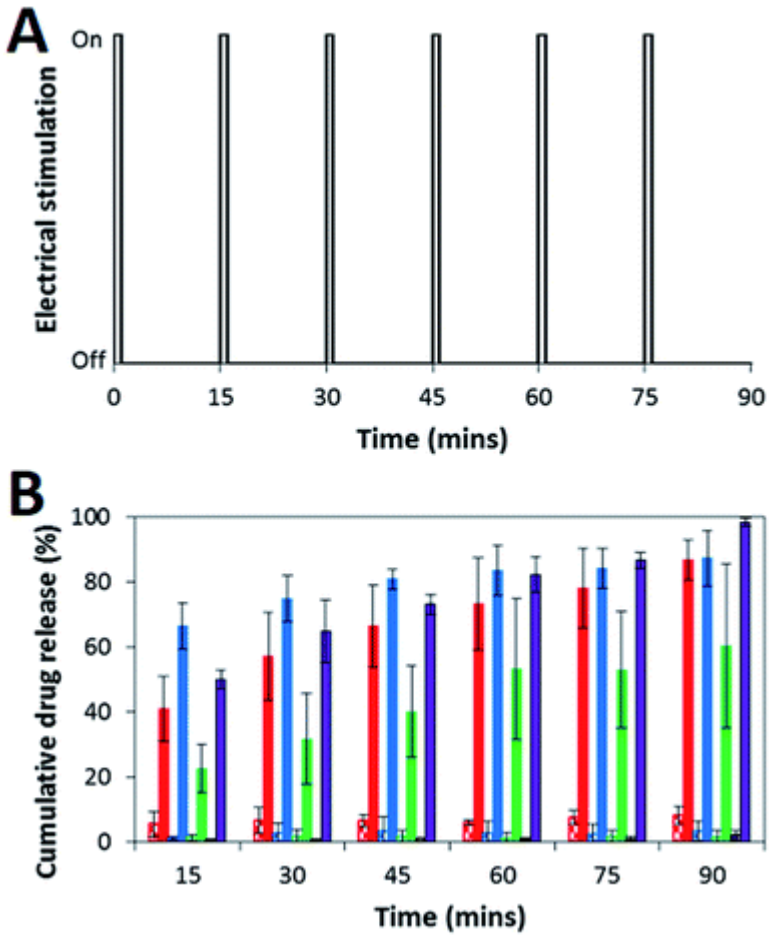

Fig. 3 Electrochemically-triggered drug delivery via potential cycling. (A) Electrical stimulation paradigm: 6 cycles of 1 minute on, 14 minutes off. (B) Release of DMP from films of **1–4** in PBS as determined by UV spectroscopy. Electrochemically-triggered DMP release (solid bars) or passive DMP release without electrical stimulation (checked bars). Polyester **1**, red. Polyester **2**, blue. Polyester **3**, green. Polyester **4**, purple.

We also studied the electrochemically-triggered release of DMP from films deposited on glass substrates. A potential step of +0.6 V was applied to each film for 30 seconds, followed by 29.5 minutes of rest (Fig. 4A) after which the quantity of DMP in solution was quantified by UV spectroscopy. The first stimulation released 5–25% of the drug from the films (Fig. 4B), the first and second stimulation released 25–50%, and the third stimulation released between 50 to 90% of the drugs from the films, all of which are clearly distinguishable from the passive release profiles (Fig. 4B and S12†).

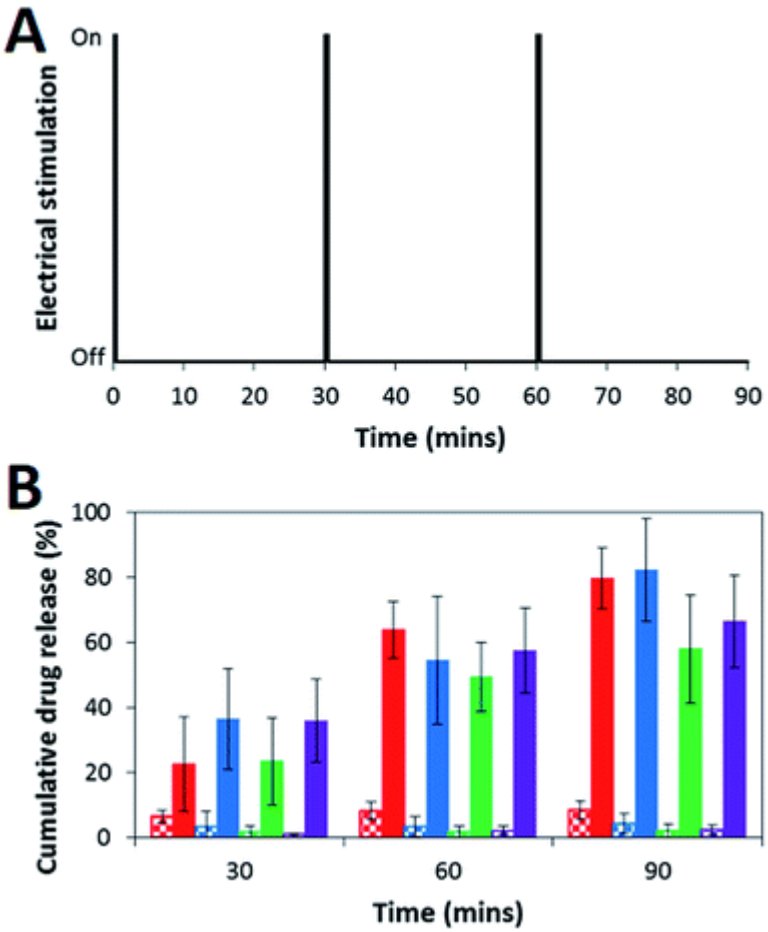

Fig. 4 Electrochemically-triggered drug delivery via a potential step. (A) Electrical stimulation paradigm: 3 cycles of 0.5 minutes on, 29.5 minutes off. (B) Release of DMP from films of **1–4** in PBS as determined by UV spectroscopy. DMP release with electrical stimulation (solid bars) or without electrical stimulation (checked bars). Polyester **1**, red. Polyester **2**, blue. Polyester **3**, green. Polyester **4**, purple.

Although it is impossible to accurately reproduce the conditions that materials encounter when implanted in vivo in the laboratory (particularly the complex tissue-specific distribution of enzymes, or patient-specific immune response), laboratory-based in vitro degradation studies are useful to confirm the potential for materials to degrade upon exposure to enzymes found in vivo. To demonstrate the susceptibility of the polymers to enzymatic/hydrolytic degradation in vitro we incubated films of polyesters **1–4** in PBS in the absence or presence of a high concentration of cholesterol esterase (4 units per mL) which is an enzyme known to hydrolyze ester bonds in polyesters.[71,117,118] We observed the mass of each film to decrease very slowly over a period of 10 days, and the presence of the esterase moderately increased the rate at which this occurs (Fig. S13†). We conclude that the films would degrade slowly if administered in vivo (over the period of several months) in line with other PEG- and PCL-based materials.[119,120]

As noted above, non-toxic FDA-approved PEG and PCL derivatives were chosen as the non-electroactive units for inclusion in the biodegradable polyesters, and degradation of the polyesters would lead to the release of low molecular weight polyethylene glycols or caprolactone derivatives that are easily cleared via the renal system. The toxicity of the electroactive oligoaniline incorporated in the polymers was first reported by Wei and co-

workers using the rat glial tumor C6 cell line, in a study that showed the aniline pentamer displays little/no cytotoxicity below 20 mg mL^{-1}, 90% cell viability at 40 mg mL^{-1}, and approximately 50% cell viability at 100 mg mL^{-1}.[121] Subsequent studies by Wei and co-workers showed the aniline pentamer to be more toxic towards adenocarcinomic human alveolar basal epithelial A549 cells, with little/no cytotoxicity below 20 μg mL^{-1}, 90% cell viability at 40 μg mL^{-1}, and approximately 50% cell viability at 100 μg mL^{-1}; furthermore, shorter oligoanilines were less cytotoxic.[86,87]

Pertinently, a study of PCL-based polyesters incorporating the aniline pentamer from Guo and Albertsson investigating the toxicity of the water soluble extracts collected after incubating the polyesters in medium typically showed human keratinocyte HaCaT cells to be ca. 90% viable using a variety of polymer compositions and architectures.[72] We adapted this methodology to investigate the toxicity of the water soluble extracts collected after incubating polyesters **1–4** in medium for 5 days, using pristine medium as a positive control experiment and pristine medium containing 15 vol% of ethanol as a negative control experiment. After exposure of human dermal fibroblast (HDF) cells to 15 vol% of ethanol we found them to be ca. 11% viable (i.e. cell viability was adversely affected), as depicted in Fig. 5. By comparison, HDFs incubated in either the pristine media or the media containing any water soluble extracts from polyesters **1–4** began to proliferate (i.e. cell viability was not adversely affected).

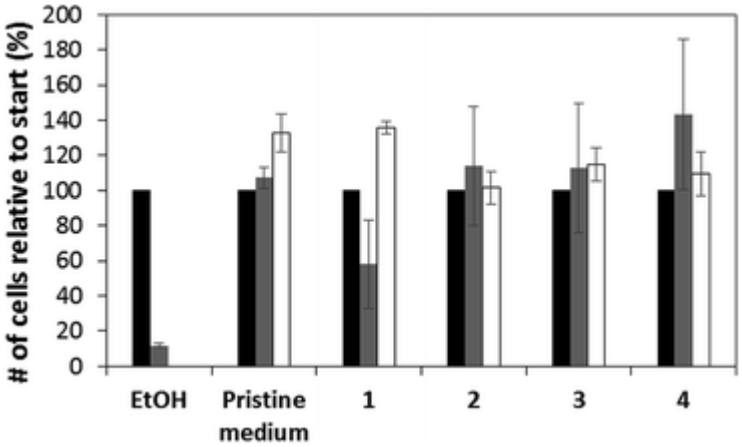

Fig. 5 Assessment of the cytocompatibility of the water soluble extracts from polyesters **1–4** incubated in media for 5 days towards human dermal fibroblasts as determined by AlamarBlue® assay. Day (0) Black bars. Day (2) Grey bars. Day (4) White bars.

Analogous CSA-doped materials have been shown to support the adhesion of a variety of cells including C6 cells,[122] keratinocytes,[72] MC3T3-E1 cells,[85] osteoblasts,[122] PC12 cells[121] and Schwann cells.[122–124] We found that films of polyesters **1** and **3** were prone to fracture as a consequence of exposure to dynamic shear forces encountered during multiple medium changes at 37 °C. Films of polyesters **2** and **4** were more robust and we observed that both HDFs and human mesenchymal stem cells (HMSCs) adhered to the surface of the films with morphologies analogous to those on commercially available conductive indium tin oxide (ITO) slides (Fig. S14†). Longer term HDF proliferation studies were complicated by poor adhesion of the films of polyesters **2** and **4** to either ITO slides or tissue-culture treated Corning® Costar® tissue culture plates, and their mechanical stability, yet HDFs were observed to adhere and remain viable over 4 days (Fig. S15†). After 8 days in culture HDFs

had proliferated on their surfaces (Fig. 6) and a LIVE/DEAD® Viability/Cytotoxicity Kit for mammalian cells demonstrated that they were highly viable (Fig. 7).

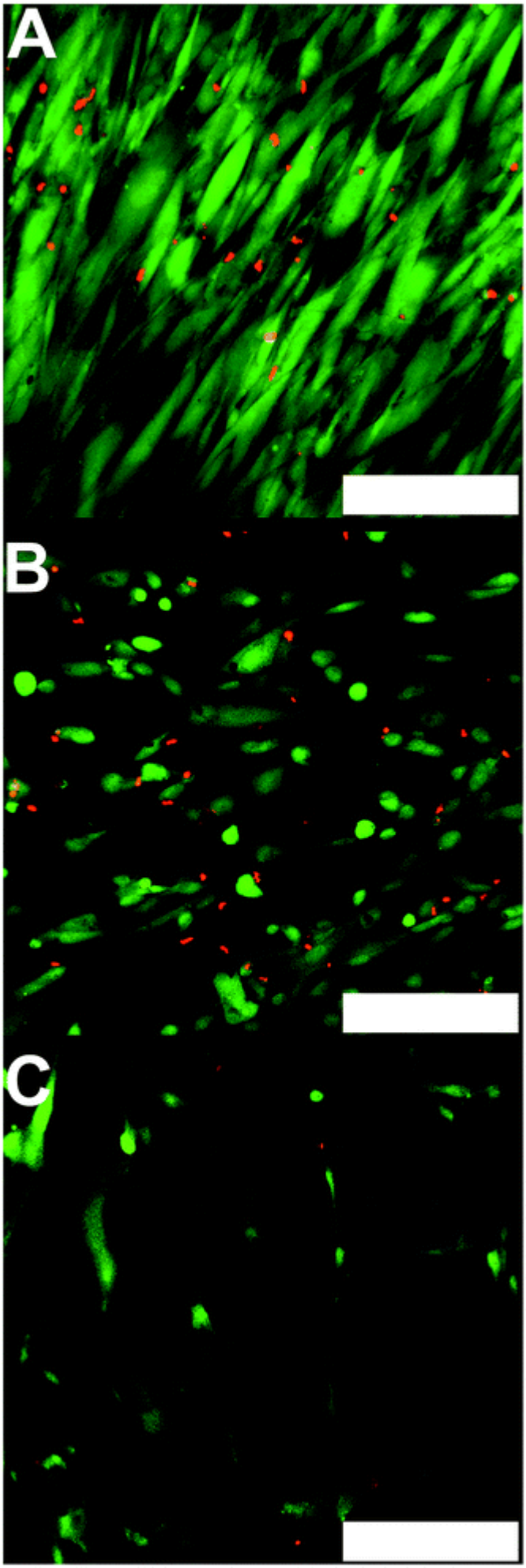
A
B
C

Fig. 6 Adhesion of human dermal fibroblasts on various surfaces after 8 days in culture. (A) Tissue-culture treated Corning® Costar® tissue culture plates. (B) CSA-doped polyester **2**. (C) CSA-doped polyester **4**. Live cells were stained green by calcein and dead cells were stained red by ethidium using a LIVE/DEAD® Viability/Cytotoxicity Kit. Scale bars represent 100 μm.

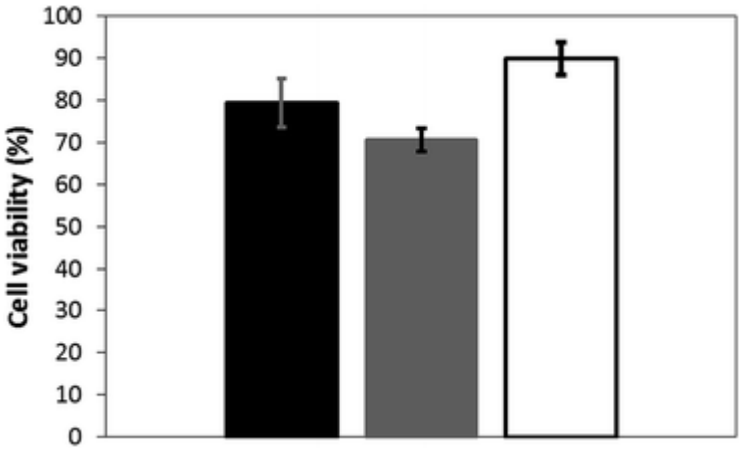

Fig. 7 Assessment of the cell viability of human dermal fibroblasts on various surfaces after 8 days in culture as determined using a LIVE/DEAD® Viability/Cytotoxicity Kit. (Black bar) Tissue-culture treated Corning® Costar® tissue culture plates. (Grey bar) CSA-doped polyester **2**. (White bar) CSA-doped polyester **4**.

Together, these results suggest that such copolymers represent valuable lead structures for the development of clinically relevant electroactive biomaterials, with potential for in vivo implantation for a variety of applications (e.g., drug eluting coatings on completely biodegradable implants).

Conclusions

Electrically triggered drug release from polyesters **1–4** provides a novel platform for drug delivery. The synthesis and purification of the polymers is simple and scalable, requiring only 3 steps from commercially available starting materials. The polymers are solution processable, thus facilitating the preparation of materials with a high drug loading of 16 or 31 wt%. Although we used the anti-inflammatory DMP as a clinically applied model drug (primarily because it is straightforward to quantify its release using UV spectroscopy), it is noteworthy that a wide variety of other biologically-active molecules (such as those for the treatment of pain) could be delivered using the stimulation paradigms described here. Furthermore, it would be possible to modulate the release profiles of these molecules via simple modifications of the electrical input, allowing the release profile to be tailored to treat the condition in the most therapeutically effective way. Both the experimental paradigms described have potential to be used for the manufacture of completely biodegradable drug delivery systems.[125] The potential cycling-induced release paradigm could be powered wirelessly.[117] The potential step-induced release paradigm could be powered using a sacrificial metal such as magnesium although this may result in the build-up of hydrogen in vivo (which can be diminished using zinc alloys).[54,126–128] A safer option to power the potential step-induced release paradigm would be the use of a biodegradable battery, which is capable of providing potentials of up to 0.6 V as used in this study.[129] The other requisite circuit components such as sensors, switches and wires could be manufactured from

biodegradable/bioerodible EAP-based materials,[130–133] all of which would be embedded within a non-conductive biodegradable polymer capsule. Moreover, the biodegradable and cytocompatible nature of the polyesters suggests that analogous materials may be of use as tissue scaffolds. Consequently, we foresee great potential for the development of biodegradable EAP-based drug delivery devices integrated into tissue scaffolds,[33,35] and, moreover, the exciting prospect of systems capable of controlling the chronopharmacology of drugs in a clinically relevant fashion.[10,30,134–136]

Experimental

Materials

Unless otherwise stated, all chemicals for synthesis and physicochemical analysis were of ACS grade, purchased from Sigma-Aldrich and used as received without further purification. Reagents for cell culture were purchased from Invitrogen (Carlsbad, CA) unless otherwise noted. Human dermal fibroblasts (HDFs) and human mesenchymal stem cells (HMSCs) were purchased from Lonza (Gaithersburg, MD). Tissue-culture treated Corning® Costar® tissue culture plates were purchased from Sigma Aldrich and pristine indium tin oxide (ITO) slides were purchased from Ted Pella, Inc. (Reading, CA).

Synthetic/analytical methods

^{1}H and ^{13}C NMR spectra were recorded on a Varian Mercury 400 MHz NMR spectrometer, using residual solvent ^{1}H peaks as internal references for the ^{1}H NMR spectra and the solvent ^{13}C peaks as references for the ^{13}C NMR spectra. The following notation is used for the ^{1}H NMR spectral splitting patterns: singlet (s), doublet (d), multiplet (m), broad (br). Mass spectra were recorded on an Agilent 6530 QTOF mass spectrometer in electrospray ionization mode. Infrared spectroscopy was carried out on a Thermo Scientific Nicolet 380 FT-IR Spectrometer (Thermo Fisher Scientific Inc., USA). Spectra were recorded in ATR mode at 21 °C, with a 1 cm^{-1} resolution and 16 scans (corrected for background and atmosphere using OMNIC software provided with the spectrometer).
Synthesis of carboxylic acid-terminated aniline pentamers (APs). The synthesis of the carboxylic acid-terminated aniline pentamers was adapted from the method of Wei and co-workers.[102]N-phenyl-1,4-phenylenediamine (9.2 g, 50 mmol) and succinic anhydride (5.0 g, 50 mmol) were dissolved in dichloromethane (300 mL) and stirred overnight at room temperature. The product was isolated by filtration, washed with diethyl ether until the diethyl ether was clear and colorless, and dried under vacuum for 24 hours, yielding 12.0 g (42 mmol, 84% yield) of blue-grey solid (a succinic acid-capped aniline dimer). This blue-grey solid (2.9 g, 10 mmol) and p-phenylenediamine (0.54 g, 5 mmol) were dissolved in dimethylformamide (DMF, 15 mL) and the solution cooled to 0 °C on ice. A cooled solution of DMF (30 mL), water (25 mL) and concentrated hydrochloric acid (5 mL) was added. A solution of ammonium persulfate (2.28 g, 10 mmol) in aqueous hydrochloric acid solution (50 mL, 1 M) was added slowly and the reaction mixture stirred quickly for 1 hour at 0 °C. After this time the reaction mixture was added to water (300 mL) resulting in the precipitation of a solid, which was isolated by filtration. The product was reduced by stirring a suspension of the product in aqueous ammonia (300 mL, 1 M) overnight, after which the pH was lowered to 2–3 by addition of aqueous hydrochloric acid (1 M), and the product isolated by filtration. The product was dried under vacuum at 45 °C for 48 hours. A solution of the crude product (3.0 g) in DMF (15 mL) was slowly added to ethanol (150 mL) resulting

in the precipitation of a solid material that was isolated by filtration and dried under vacuum. The product was purified by Soxhlet extraction with 1,2-dichloroethane followed by THF. The succinic acid-capped aniline pentamer (AP) (Scheme S1†) was dried under vacuum for 48 hours, after which 1.8 g (2.7 mmol, 54% yield) was isolated in an analytically pure form in accordance with the literature.[102] ^{1}H NMR (400 MHz, DMSO-d_6) δ_H 9.80 (s, 2H, CONH), 7.46–7.44 (m, 4H, Ar-H), 7.36 (s, 2H, Ar-H), 7.23 (s, 2H, Ar-H), 7.18 (m, 4H, Ar-H), 7.11 (s, 2H, Ar-H), 7.04–6.95 (m, 6H, Ar-H), 2.62–2.55 (m, 8H, CH_2); ^{13}C NMR (100 MHz, DMSO-d_6) δ_C 177.24 (COOH), 173.94 (CONH), 140.81 (Ar-C), 138.30 (Ar-C), 137.12 (Ar-C), 135.65 (Ar-C), 132.32 (Ar-C), 120.44 (Ar-C), 119.47 (Ar-C), 118.36 (Ar-C), 117.50 (Ar-C), 115.38 (Ar-C), 31.00 (CH_2), 29.21 (CH_2). ESI-MS (m/z) calculated for $C_{38}H_{35}N_6O_6$ $[M + H]^+$ requires 672.25; found, 672.25. IR (ATR) ν_{max} cm^{-1} 3293 (NH, amide), 1712 (C=O, acid).

General methodology for the synthesis of the electroactive polyesters. The synthesis of the electroactive polyesters adapted from the method of Wei and co-workers.[81] In short, alcohol-terminated poly(ethylene glycol)s or poly(caprolactone)s (3 mmol) were dissolved in N-methyl-2-pyrrolidone (NMP, 20 mL), to which was added AP (2.0 g, 3.0 mmol), dicyclohexylcarbodiimide (DCC, 1.9 g, 9.0 mmol) and 4-dimethylaminopyridine (DMAP, 0.2 g, 2.0 mmol). The reaction mixture was stirred at room temperature under an inert atmosphere of argon. After 72 hours the reaction mixture was filtered and added drop-wise to diethyl ether (1.5 L) that was stirred to assure the precipitation of a fine powder of the respective polymer. The stir bar was removed and the product was allowed to settle to the bottom of the container (typically 15–30 minutes). The diethyl ether was removed via pipette suction, and the polymer-rich layer at the bottom of the container was concentrated with a rotary evaporator to yield a thick oil. The oil was dissolved/dispersed in chloroform (10 mL), after which it was re-precipitated in diethyl ether, and this process of resuspension in chloroform followed by re-precipitation in diethyl ether was repeated two more times. The resulting polymers were dried under high vacuum for 24 hours. The polymers could be reduced to the leucoemeraldine state via brief exposure to aqueous hydrazine for ca. 15 minutes (after which no further gas was observed to evolve) followed by dialysis against ultrapure water in a cellulose dialysis tube with a molecular weight cutoff of ca. 3500 Da, and dried under high vacuum for 48 hours.

Synthesis of electroactive polyester **1**. Polyester **1** was synthesized using poly(ethylene glycol) with an average molecular weight of 400 Da, and 1.6 g of **1** (Scheme 1) was isolated via this procedure, in a yield of 50% by mass. ^{1}H NMR (400 MHz, DMSO-d_6): δ_H = 10.20 (br s, CONH), 9.90 (br s, CONH), 7.68 (br, NH), 7.53–7.45 (m, Ar-H), 7.36 (s, Ar-H), 7.24 (d, Ar-H), 7.19–6.90 (m, Ar-H), 3.75–3.55 (m, CH_2O), 3.52–3.48 (m, CH_2O), 2.62–2.55 (m, CH_2); ^{13}C NMR (100 MHz, DMSO-d_6): δ_C = 174.3 (CO_2R), 173.9 (CONH), 173.7 (CONH), 140.7 (Ar-C), 138.3 (Ar-C), 137.6 (Ar-C), 135.5 (Ar-C), 134.3 (Ar-C), 126.4 (Ar-C), 125.1 (Ar-C), 120.44 (Ar-C), 119.2 (Ar-C), 118.8 (Ar-C), 117.5 (Ar-C), 115.4 (Ar-C), 72.7 (CH_2O), 70.2 (CH_2O), 25.0 (CH_2), 24.7 (CH_2). IR (ATR) ν_{max} cm^{-1} 3293 (NH, amide), 1732 (C=O, ester).

Synthesis of electroactive polyester **2**. Polyester **2** was synthesized using alcohol-terminated poly(ethylene glycol)s with an average molecular weight of 2000 Da, and 4.25 g of **2** (Scheme 1) was isolated via this procedure, in a yield of 53% by mass. ^{1}H NMR (400 MHz, DMSO-d_6): δ_H = 10.20 (br s, CONH), 9.90 (br s, CONH), 7.68 (br, NH), 7.53–7.45 (m, Ar-H), 7.36 (s, Ar-H), 7.24 (d, Ar-H), 7.19–6.90 (m, Ar-H), 3.75–3.55 (m, CH_2O), 3.52–3.48 (m, CH_2O), 2.62–2.55 (m, CH_2); ^{13}C NMR (100 MHz, DMSO-d_6): δ_C solubility too low. IR (ATR) ν_{max} cm^{-1} 3293 (NH, amide), 1732 (C=O, ester).

Synthesis of electroactive polyester **3**. Polyester **3** was synthesized using poly(caprolactone) diol with an average molecular weight of 530 Da, and 2.2 g of **3** (Scheme 2) was isolated via this procedure, in a yield of 62% by mass. ^{1}H NMR (400 MHz, DMSO-d_6) δ_H 10.19 (s,

CONH), 9.89 (s, CONH), 7.68 (br, NH), 7.53–7.45 (m, Ar-H), 7.35 (s, Ar-H), 7.22 (d, Ar-H), 7.19–6.90 (m, Ar-H), 4.11 (m, CH_2O, PCL), 3.75–3.55 (m, CH_2O, diethyleneglycol spacer), 3.52–3.48 (m, CH_2O, diethyleneglycol spacer), 2.69–2.55 (m, CH_2), 1.66 (m, CH_2), 1.55 (m, CH_2), 1.29 (m, CH_2); ^{13}C NMR (100 MHz, DMSO-d_6) δ_C 174.4 (CO_2R), 174.2 (CO_2R), 173.2 (CONH), 140.7 (Ar-C), 138.3 (Ar-C), 137.6 (Ar-C), 135.5 (Ar-C), 134.3 (Ar-C), 126.4 (Ar-C), 125.1 (Ar-C), 120.44 (Ar-C), 119.2 (Ar-C), 118.8 (Ar-C), 117.5 (Ar-C), 115.4 (Ar-C), 70.2 (CH_2O, diethyleneglycol spacer), 68.7 (CH_2O, diethyleneglycol spacer), 63.9 (CH_2O, PCL), 33.8 (CH_2), 32.6 (CH_2), 32.3 (CH_2), 31.4 (CH_2), 30.6 (CH_2), 29.4 (CH_2), 28.2 (CH_2), 25.3 (CH_2), 25.0 (CH_2), 24.7 (CH_2). IR (ATR) ν_{max} cm^{-1} 3293 (NH, amide), 1732 (C=O, ester).
Synthesis of electroactive polyester **4**. Polyester **4** was synthesized using poly(caprolactone) diol with an average molecular weight of 2000 Da, and 1.0 g of **4** (Scheme 2) was isolated via this procedure, in a yield of 25% by mass. ^{1}H NMR (400 MHz, DMSO-d_6): δ_H = 10.19 (s, CONH), 9.89 (s, CONH), 7.68 (br, NH), 7.53–7.45 (m, Ar-H), 7.35 (s, Ar-H), 7.22 (d, Ar-H), 7.19–6.90 (m, Ar-H), 4.11 (m, CH_2O, PCL), 3.75–3.55 (m, CH_2O, diethyleneglycol spacer), 3.52–3.48 (m, CH_2O, diethyleneglycol spacer), 2.69–2.55 (m, CH_2), 1.66 (m, CH_2), 1.55 (m, CH_2), 1.29 (m, CH_2); ^{13}C NMR (100 MHz, DMSO-d_6): solubility too low. IR (ATR) ν_{max} cm^{-1} 3293 (NH, amide), 1732 (C=O, ester).

Film preparation and characterization

Film preparation. Films were prepared by casting solutions of the polymers in hexafluoroisopropanol (HFIP, typically 0.1 g mL^{-1}) onto HFIP insoluble substrates, (e.g., microscope slides with dimensions of 2.5 cm × 5 cm or glassy carbon electrodes with surface areas of 0.0314 cm^2). The solvent was allowed to evaporate in a fume hood, and the films were subsequently dried under vacuum for 48 hours at room temperature. The polymers were doped by the addition of camphorsulfonic acid (CSA) to the HFIP solution prior to casting on microscope slides. Unless otherwise stated CSA doping was at a mole ratio of 3 : 1 CSA : AP.[72]
Profilometry. Profilometry was carried out using a Veeco Dektak 6M Stylus Profilometer (Veeco Instruments Inc., NY) fitted with a 12.5 μm stylus tip. The profilometer was isolated on an air table to reduce ambient vibrations. The profilometer was operated at 10 mg of stylus force, and used to record profiles of distances of ca. 1 cm, recording data points every 555 nm. Data analysis was carried out with the software provided by the manufacturer, which allowed the determination of the thickness and roughness of the films. The surface roughness parameters are analyzed and reported in accordance with the ISO 25178 series. The average roughness (R_a) is the arithmetic average of the deviation from the mean line, and is the most used international parameter of roughness, and the root-mean-square roughness (R_q) is based upon this. The average height difference between the five highest peaks and the five lowest valleys (R_zDIN) was determined in accordance with DIN 4768/1 as specified by the Deutsches Institut für Normung. Doping the films with CSA altered the surface roughness in all cases because protonation of the oligoaniline blocks by the CSA caused rearrangement of the polymers on the nanoscale.[104]
Conductivity determination. The conductance of films of **1–4** were measured in accordance with protocol IPC-TM-650, number 2.5.17.2 described by the Institute for Interconnecting and Packaging Electronic Circuits. Films supported on glass slides were examined by chronoamperometry using a CHI900C electrochemical workstation (CHI instruments, Austin, TX). Chronoamperometric measurements were made with a two-point probe system (copper alligator clips), by connecting counter and reference electrodes together. Briefly, two thin strips of adhesive-backed copper tape (Ted Pella, Inc., Redding, CA) were attached to the films, parallel to one another, separated by a distance of 0.5 cm. The working and counter

electrodes were clipped on the strips of copper tape, and the current measured for 50 seconds during a potential step experiment at 10 V. The electrodes were moved to different positions after each measurement, and the current passed was recorded in at least five different positions. The resistance (R, Ω) of the films was determined in accordance with eqn (1):

$$R = V/I \quad (1)$$

The resistivity (Ω cm^{-1}) of the films was determined in accordance with eqn (2):

$$\rho = Rwt/L \quad (2)$$

In which: w corresponds to the width of the film in cm (2.5 cm); t corresponds to the thickness of the film in cm (as determined via profilometry); and L corresponds to the length of the film in cm (0.5 cm). The conductivity (S cm^{-1}) of the films was determined in accordance with eqn (3):

$$\sigma = 1/\rho \quad (3)$$

Differential scanning calorimetry (DSC). DSC experiments were carried out with a DSC Q100 (TA Instruments, USA), using airtight aluminum pans. Films were precisely weighed into aluminum pans (TA Instruments, USA), and analyses were carried out under a nitrogen atmosphere (flow rate of 50 mL min^{-1}). The samples were treated as follows: heated from room temperature to 200 °C (10 °C min^{-1}), cooled to 0 °C (10 °C min^{-1}), heated from 0 °C to 200 °C (5 °C min^{-1}), cooled to 0 °C (5 °C min^{-1}), heated from 0 °C to 200 °C (10 °C min^{-1}), and finally cooled to 0 °C (10 °C min^{-1}).

Thermogravimetric analysis (TGA). TGA was conducted on a TA Instruments TGA Q500 thermogravimetric analyzer (TA Instruments, USA), using a ramp rate of (10 °C min^{-1}) under nitrogen gas. Weight loss from the polymers occurring below 200 °C was ascribed to the evaporation of solvents, and above 200 °C it was ascribed to the decomposition of the polymers. The polyesters synthesized via the condensation of AP with low molecular weight diols, polymers **1** (PEG of ca. 400 Da) and **3** (PCL of ca. 530 Da) respectively, were observed to decompose in two steps, first the diol blocks decomposed between 200–300 °C, followed by the decomposition of AP above this temperature. By comparison, those polyesters synthesized via the condensation of AP with higher molecular weight diols, polymers **2** (PEG of ca. 2000 Da) and **4** (PCL of ca. 2000 Da) respectively, displayed somewhat greater thermal stabilities, and the diol blocks decomposed between 200–410 °C, followed by the decomposition of the aniline pentamer above this temperature.[78]

UV-visible absorption spectra of films. UV-visible absorption spectra of very thin films supported on quartz microscope slides (with dimensions of 2.5 cm × 1 cm, supplied by Ted Pella, Inc.) were recorded at room temperature on a Beckman Coulter DU720 general purpose UV-visible spectrophotometer (Beckman Coulter Inc., CA).

Voltammetry. Voltammetry experiments were carried out using a CHI6273C electrochemical analyzer (CH Instruments, Inc.). Polymers (5 mg) were dissolved in DMSO (0.5 mL), doped with hydrochloric acid (HCl, 50 μL, 1 M), added to deoxygenated phosphate buffered saline (PBS, 50 mL, pH 7.0) that was prepared by bubbling nitrogen through it for 10 minutes. The mixture was stirred for 5 minutes under nitrogen prior to filtration to remove the stir bar and any insoluble polymer before the electrochemical measurements were made. A three-

electrode system consisting of two Pt meshes as working and counter electrodes, and an Ag/AgCl reference electrode. Unless otherwise stated, the scan rate was 20 mV s^{-1}. Solutions of the polyesters were metastable, and there was evidence of aggregation of the polymers within the duration of the experiment. Those polymers incorporating polyethylene glycol chains between the oligoanilines (**1** and **2**) were somewhat less prone to aggregation than those incorporating polycaprolactone chains between the oligoanilines (**3** and **4**).
X-ray diffraction (XRD). XRD data was collected on a Rigaku R-Axis Spider diffractometer with an image plate detector using a graphite monochromator with CuKα radiation (λ = 1.5418 Å) at room temperature. The instrument was controlled using Rapid/XRD diffractometer control software (Rapid/XRD Version 2.3.8., Rigaku Americas Corporation, The Woodlands, TX). The integration of the two dimensional data into a one dimensional pattern was accomplished using 2DP (2DP Version 1.0., Rigaku Americas Corporation, The Woodlands, TX). Percentage crystallinities were determined by taking the ratio of the crystalline area to the amorphous area in the XRD spectrum. Areas were determined by profile fitting of the crystalline peaks and amorphous humps. A constant linear background was used in the profile fitting to eliminate potential variations in area determination caused by subjective selection of shape and level. All XRD pattern analysis was performed using JADE software (MDI, v 8.1).

In vitro drug delivery, degradation and cell culture studies

Preparation of drug doped films. Films of ca. 3–4 mg were prepared by casting solutions of **1–4** and DMP (at a mole ratio of 1 : 1 DMP : AP) in hexafluoroisopropanol (typically 0.1 g mL^{-1}) onto a glassy carbon electrode (0.0314 cm^2, CH Instruments, Inc.) or a glass slide. The solvent was allowed to evaporate in a fume hood, and the films were subsequently dried under vacuum for 48 hours at 60 °C.
Drug delivery studies. Voltammetry experiments were carried out using a CHI6273C electrochemical analyzer (CH Instruments, Inc.). Phosphate buffered saline (PBS, pH 7.0) was deoxygenated for 10 minutes with argon before the electrochemical measurements were made.

Electrochemically-triggered release (i.e., de-doping) of DMP from the films deposited on glassy carbon substrates by potential cycling, was achieved using a three-electrode system consisting of one polymer film-coated glassy carbon working electrode, a Pt mesh counter electrode, and an Ag/AgCl reference electrode in 4 mL PBS. Prior to each experiment there was a 10 s “quiet time”, the initial potential was 0 V, the high potential was 0.7 V, the low potential was −0.5 V, the initial scan was positive, the current was measured at intervals of 0.001 V, the scan rate used in all experiments was 50 mV s^{-1}, and this stimulation lasted 62 seconds. The films were allowed to rest for 14 minutes after which the quantity of DMP in solution was quantified by UV spectroscopy. The medium was unchanged between cycles, and the data are reported as cumulative release as a percentage of the total mass of drug in the film over the period of the experiment. These data are compared to passive DMP release from unstimulated films measured every 15 minutes. For experiments using multiple scans, a scan from 0.7 V to −0.5 V and back to 0.7 V was regarded as one additional cycle and each cycle lasted 48 seconds (see Fig. S7–S10†).

Electrochemically-triggered release (i.e., de-doping) of DMP from films deposited on glass substrates using a potential step was achieved by connecting two thin strips of adhesive-backed copper tape (Ted Pella, Inc.) were attached to the films, parallel to one another, separated by a distance of 1.1 cm. The counter and reference electrodes were connected

together and clipped to copper tape on one side of the film, and the working electrode was clipped to copper tape on the other side of the film. A polycarbonate well with a square hole (sides of 0.9 cm) was attached to the film and copper tape using vacuum grease and binder clips to assure a firm seal, with PBS (0.5 mL) added to the well. A potential step of +0.6 V was applied to each film for 30 seconds, followed by 29.5 minutes of rest after which the concentration of DMP in solution was quantified by UV spectroscopy.

DMP release was quantified by UV spectroscopy using a BioTek Epoch® plate reader (BioTek US, Winooski, VT) equipped with a Take3 Micro-volume Plate and Gen5 v2.04 Software supplied with the plate reader. Two samples of 2 μL were removed from the release medium at specific time points and absorbance readings were carried out at 242 nm (the characteristic absorbance band of DMP). Absorptions were corrected by subtracting the reading of PBS alone from each sample. A standard calibration curve for DMP was plotted to define the quantitative relationship between the observed absorbance and the concentration of DMP. Prior to the experiment, the mass of the drug-doped polymer film on the substrate was determined by subtracting the mass of the substrate from the mass of the polymer-coated substrate. Data are plotted as % DMP release relative to the quantity of DMP theoretically in the film at the beginning of the experiment, and all data are the average of at least three samples.

Degradation studies. Films (of ca. 4 mg) were incubated in PBS (1 mL) at 25 °C, in the absence or presence of cholesterol esterase (4 units per mL, Sigma Aldrich, USA). At specific time points the buffer was removed, the films were carefully washed with deionized water, and the films were then dried under high vacuum for 22 hours, after which the mass of the film was determined on a high precision balance. The buffer (with or without enzymes) was replaced, and the mass of the film was recorded over a period of several days. Films were undoped to help differentiate degradation from dopant leaching. The mass loss profiles are the average of at least three samples.
Studies of the cytotoxicity of the degradation products of the polymers. The polymers (200 mg) were sterilized by incubation in 70% ethanol solution, followed by exposure to UV for 30 minutes and allowed to dry in a sterile tissue culture hood overnight. The polymers were subsequently incubated for 5 days at 37 °C in 2 mL of HDF/HMSC growth medium was composed of: high glucose Dulbecco's Modified Eagle Medium (DMEM, 440 mL); fetal bovine serum (50 mL); antibiotic–antimycotic (5 mL); non-essential amino acids (5 mL), and 2 ng mL^{-1} basic fibroblast growth factor. The media was filtered using a sterile Millipore 220 nm syringe filter and used for subsequent cell culture experiments as follows.

Commercially available tissue-culture treated Corning® Costar® 96 well tissue culture plates were used as substrates upon which HDF cells were seeded at 10 000 cells per cm^2 under 100 μL of medium (one of the following: medium that had previously been incubated with the polymers; pristine medium as a positive control experiment; or pristine medium containing 15 vol% ethanol as a negative control experiment), and incubated at 37 °C, 95% humidity, and a CO_2 content of 5%.

After 2 days the cells were washed gently with PBS, followed by the addition of pristine medium containing 10% v/v of the AlamarBlue® reagent. After 2.5 hours of culture, the medium was aspirated and replaced with medium (either medium that had previously been incubated with the polymers, or pristine medium for control experiments). The aspirated medium containing the AlamarBlue® reagent was placed in another 96 well plate, and the fluorescence was measured with a fluorimeter (Synergy HT Multi-Mode Microplate Reader,

Biotek US, Winooski, VT). Two controls were considered during the measurement of the fluorescence: the first was wells containing medium alone (i.e. no cells or AlamarBlue® reagent), which was not fluorescent; and the second was wells that contained the AlamarBlue® reagent but no cells (used for baseline correction). Numbers of cell adhered to the various surfaces studied herein are reported relative to their initial seeding density of 10 000 cells per cm^2, which was assigned an arbitrary value of 100%. After another 2 days (i.e. at 4 days after initial seeding) the AlamarBlue® assay was repeated. Results presented are the average of eight samples.

Cell adhesion studies. Commercially available conductive ITO slides were used for control experiments. Clean ITO slides and ITO slides coated with polyester films doped with CSA (at a mole ratio of 1 : 1 CSA : AP) were inserted in tissue culture plates and sterilized by incubation in 70% ethanol solution, followed by exposure to UV for 30 minutes. After sterilization, the slides (coated and uncoated) were incubated for 30 minutes under 3 mm of medium. HDF/HMSC growth medium was composed of: high glucose Dulbecco's Modified Eagle Medium (DMEM, 440 mL); fetal bovine serum (50 mL); antibiotic–antimycotic (5 mL); non-essential amino acids (5 mL), and 2 ng mL^{-1} basic fibroblast growth factor. Medium was aspirated and replaced prior to HDF or HMSC seeding. Cell viability before starting the experiment was determined by the Trypan Blue (Sigma, USA) exclusion method, and the measured viability exceeded 95% in all cases. Cells were seeded at 10 000 cells per cm^2 under 3 mm of medium, and incubated at 37 °C, 95% humidity, and a CO_2 content of 5%. After 2 days the medium was aspirated and the films were washed gently with PBS. Cells were fixed with 4% paraformaldehyde in PBS for 15 min, permeabilized with 0.1% Triton X-100 (Fluka) and 2% bovine serum albumin (BSA) in PBS buffer for 5 min, followed by blocking with 2% BSA in PBS buffer for 30 min at room temperature. Actin filaments and cell nuclei within cells were stained with Alexa Fluor 488® Phalloidin (Life Technologies, USA) for 30 min and 4′,6-diamidino-2-phenylindole (DAPI, Invitrogen, USA) for 5 min. The cells were then washed three times with PBS buffer and stored at 4 °C until images were acquired. Fluorescence images of cells were captured using a colour CCD camera (Optronics® MagnaFire, Goleta, CA, USA) attached to a fluorescence microscope (IX-70; Olympus America Inc.). Images are representative of 3 samples.
Cell proliferation studies. The cell proliferation studies were carried out in accordance with previously reported methodology[137,138] employing the AlamarBlue® assay. Commercially available tissue-culture treated Corning® Costar® tissue culture plates were used for control experiments. Polyester films doped with CSA (at a mole ratio of 1 : 1 CSA : AP) were cast in tissue culture plates, dried under high vacuum for 48 hours at room temperature and sterilized by incubation in 70% ethanol solution, followed by exposure to UV for 30 minutes. After sterilization, films were incubated for 30 minutes under 3 mm of medium. HDF/HMSC growth medium was composed of: high glucose Dulbecco's Modified Eagle Medium (DMEM, 440 mL); fetal bovine serum (50 mL); antibiotic–antimycotic (5 mL); non-essential amino acids (5 mL), and 2 ng mL^{-1} basic fibroblast growth factor. Medium was aspirated and replaced prior to HDF seeding. Cell viability before starting the experiment was determined by the Trypan Blue (Sigma, USA) exclusion method, and the measured viability exceeded 95% in all cases. Cells were seeded at 10 000 cells per cm^2 under 3 mm of medium, and incubated at 37 °C, 95% humidity, and a CO_2 content of 5%.

After 2 days the cells were washed gently with PBS, followed by the addition of fresh medium containing 10% v/v of the AlamarBlue® reagent. After 2.5 hours of culture, the medium was aspirated and replaced with fresh medium, and 100 μL of the aspirated medium containing the AlamarBlue® reagent was placed in a 96 well plate, and the fluorescence was

measured with a fluorimeter (Synergy HT Multi-Mode Microplate Reader, Biotek US, Winooski, VT). Two controls were considered during the measurement of the fluorescence: the first was wells containing medium alone (i.e. no cells or AlamarBlue® reagent), which was not fluorescent; and the second was wells that contained the AlamarBlue® reagent but no cells (used for baseline correction). Numbers of cell adhered to the various surfaces studied herein are reported relative to their initial seeding density of 10 000 cells per cm^2, which was assigned an arbitrary value of 100%. After another 2 days (i.e. at 4 days after initial seeding) this process was repeated. The medium was aspirated and replaced once more at 6 days after initial seeding, and finally after a total of 8 days in culture the viability of the cells was evaluated using a LIVE/DEAD® Viability/Cytotoxicity Kit for mammalian cells (Molecular Probes, Eugene, OR). The medium was removed and cells on the surfaces were incubated with 4 μM ethidium and 2 μM calcein AM in PBS for 15 min at 37 °C in the dark. Live cells were stained green because of the cytoplasmic esterase activity, which results in reduction of calcein AM into fluorescent calcein, and dead cells were stained red by ethidium, which enters the cells via damaged cell membranes and becomes integrated into the DNA strands. Fluorescence images of cells were captured using a color CCD camera (Optronics® MagnaFire, Goleta, CA, USA) attached to a fluorescence microscope (IX-70; Olympus America Inc.). Cells were counted with the cell counter tool (plugin) in the open source program ImageJ, all cells on all images were counted. Results of AlamarBlue® assays presented are the average of four samples and ethidium/calcein stained images are representative of 3 samples.

Acknowledgements

We thank Andrea P. Carranza, YoungIn Jun, Min Joo Sohn and Pei-Yun Tseng for early work related to the synthesis of well-defined oligomers of aniline, and David Aguilar Jr for assistance with early work related to the drug delivery studies. We thank the University of Texas at Austin for financial support of Jong Min Kim, David James Mouser and Min Joo Sohn in the form of Undergraduate Research Fellowships. At the Department of Chemistry at the University of Texas at Austin we thank Prof. Christopher W. Bielawski for the loan of quartz cuvettes for dynamic light scattering experiments, Dr Karin M. Keller and Dr Ian Riddington for electrospray ionization mass spectra, Prof. Michael J. Krische for access to an IR spectrometer, Prof. C. Grant Willson for access to DSC and TGA apparatus, and Dr Vincent M. Lynch for assistance with X-ray diffraction data collection. At the Department of Chemical Engineering at the University of Texas at Austin we thank Chase Cornellison for assistance with image processing. We thank the National Science Foundation for Grant no. 0741973 that was used to purchase the Rigaku R-Axis Spider diffractometer. We thank Dr Yohannes H. Rezenom of the Laboratory for Biological Mass Spectrometry in the Department of Chemistry at Texas A&M University in College Station, TX, for MALDI-TOF mass spectra. We thank the University of Florida for financial support in the form of startup resources.

Notes and references

1. A. S. Mandal, N. Biswas, K. M. Karim, A. Guha, S. Chatterjee, M. Behera and K. Kuotsu, J. Controlled Release, 2010, 147, 314 CrossRef CAS PubMed  .
2. M. H. Smolensky and N. A. Peppas, Adv. Drug Delivery Rev., 2007, 59, 823 CrossRef CAS PubMed  .
3. B. Chertok, M. J. Webber, M. D. Succi and R. Langer, Mol. Pharm., 2013, 10, 3531 CAS Search PubMed  .
4. R. Dallmann, S. A. Brown and F. Gachon, Annu. Rev. Pharmacol. Toxicol., 2014, 54, 339 CrossRef CAS PubMed  .
5. M. E. Caldorera-Moore, W. B. Liechty and N. A. Peppas, Acc. Chem. Res., 2011, 44, 1061 CrossRef CAS PubMed  .
6. C. L. Bayer and N. A. Peppas, J. Controlled Release, 2008, 132, 216 CrossRef CAS PubMed  .

7. M. Rosbash, PLoS Biol., 2009, 7, e1000062 CrossRef PubMed .
8. J. A. Evans and A. J. Davidson, Prog. Mol. Biol. Transl. Sci., 2013, 119, 283 Search PubMed .
9. F. Levi and U. Schibler, Annu. Rev. Pharmacol. Toxicol., 2007, 47, 593 CrossRef CAS PubMed .
10. S. Ohdo, S. Koyanagi and N. Matsunaga, Adv. Drug Delivery Rev., 2010, 62, 885 CrossRef CAS PubMed .
11. B.-B. C. Youan, Adv. Drug Delivery Rev., 2010, 62, 898 CrossRef CAS PubMed .
12. S. Sukumaran, R. R. Almon, D. C. DuBois and W. J. Jusko, Adv. Drug Delivery Rev., 2010, 62, 904 CrossRef CAS PubMed .

13. P. F. Innominato, F. A. Lévi and G. A. Bjarnason, Adv. Drug Delivery Rev., 2010, 62, 979 CrossRef CAS PubMed  .
14. B. R. Gandhi, A. S. Mundada and P. P. Gandhi, Drug Delivery, 2011, 18, 1 CrossRef CAS PubMed  .
15. C. Vauthier and D. Labarre, J. Drug Delivery Sci. Technol., 2008, 18, 59 CAS Search PubMed  .
16. O. Onaca, R. Enea, D. W. Hughes and W. Meier, Macromol. Biosci., 2009, 9, 129 CrossRef CAS PubMed  .
17. S. Mura, J. Nicolas and P. Couvreur, Nat. Mater., 2013, 12, 991 CrossRef CAS PubMed  .
18. R. Lehner, X. Y. Wang, S. Marsch and P. Hunziker, J. Nanomed. Nanotechnol., 2013, 9, 742 CrossRef CAS PubMed  .

19. C. Jerome, MRS Bull., 2010, 35, 665 CrossRef CAS Search PubMed  .
20. S. Ganta, H. Devalapally, A. Shahiwala and M. Amiji, J. Controlled Release, 2008, 126, 187 CrossRef CAS PubMed  .
21. E. Fleige, M. A. Quadir and R. Haag, Adv. Drug Delivery Rev., 2012, 64, 866 CrossRef CAS PubMed  .
22. B. P. Timko, K. Whitehead, W. W. Gao, D. S. Kohane, O. Farokhzad, D. Anderson and R. Langer, Annu. Rev. Mater. Res., 2011, 41, 1 CrossRef CAS Search PubMed  .
23. D. S. Kohane and R. Langer, Chem. Sci., 2010, 1, 441 RSC  .
24. T. Hoare, B. P. Timko, J. Santamaria, G. F. Goya, S. Irusta, S. Lau, C. F. Stefanescu, D. B. Lin, R. Langer and D. S. Kohane, Nano Lett., 2011, 11, 1395 CrossRef CAS PubMed  .

25. T. Cohen-Karni, R. Langer and D. S. Kohane, ACS Nano, 2012, 6, 6541 CrossRef CAS PubMed  .
26. S. Venkatesh, M. E. Byrne, N. A. Peppas and J. Z. Hilt, Expert Opin. Drug Delivery, 2005, 2, 1085 CrossRef CAS PubMed  .
27. M. Caldorera-Moore and N. A. Peppas, Adv. Drug Delivery Rev., 2009, 61, 1391 CrossRef CAS PubMed  .
28. N. A. Peppas, Adv. Drug Delivery Rev., 2013, 65, 5 CrossRef CAS PubMed  .
29. P. Mali, N. Bhattacharjee and P. C. Searson, Nano Lett., 2006, 6, 1250 CrossRef CAS PubMed  .
30. N. A. Peppas and W. Leobandung, J. Biomater. Sci., Polym. Ed., 2004, 15, 125 CrossRef CAS PubMed  .

31. A. D. Bendrea, L. Cianga and I. Cianga, J. Biomater. Appl., 2011, 26, 3 CrossRef CAS PubMed  .
32. N. K. Guimard, N. Gomez and C. E. Schmidt, Prog. Polym. Sci., 2007, 32, 876 CrossRef CAS PubMed  .
33. J. G. Hardy, J. Y. Lee and C. E. Schmidt, Curr. Opin. Biotechnol., 2013, 24, 847 CrossRef CAS PubMed 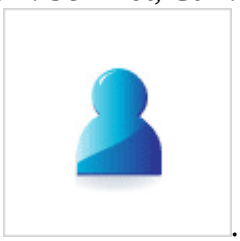 .
34. C. E. Schmidt, V. R. Shastri, J. P. Vacanti and R. Langer, Proc. Natl. Acad. Sci. U. S. A., 1997, 94, 8948 CrossRef CAS Search PubMed  .
35. B. L. Guo, L. Glavas and A. C. Albertsson, Prog. Polym. Sci., 2013, 38, 1263 CrossRef CAS PubMed 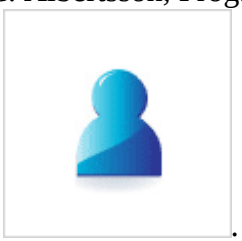 .
36. M. Ates, T. Karazehir and A. Sezai Sarac, Curr. Phys. Chem., 2012, 2, 224 CrossRef CAS Search PubMed  .

37. P. Leclere, M. Surin, P. Jonkheijm, O. Henze, A. P. H. J. Schenning, F. Biscarini, A. C. Grimsdale, W. J. Feast, E. W. Meijer, K. Mullen, J. L. Bredas and R. Lazzaroni, Eur. Polym. J., 2004, 40, 885 CrossRef CAS PubMed  .
38. V. Saxena and B. D. Malhotra, Curr. Appl. Phys., 2003, 3, 293 CrossRef Search PubMed  .
39. J. N. Barisci, T. W. Lewis, G. M. Spinks, C. O. Too and G. G. Wallace, J. Intell. Mater. Syst. Struct., 1998, 9, 723 CrossRef CAS PubMed  .
40. M. R. Abidian and D. C. Martin, Adv. Funct. Mater., 2009, 19, 573 CrossRef CAS PubMed  .
41. K. Svennersten, K. C. Larsson, M. Berggren and A. Richter-Dahlfors, Biochim. Biophys. Acta, 2011, 1810, 276 CrossRef CAS PubMed  .
42. K. Tybrandt, K. C. Larsson, S. Kurup, D. T. Simon, P. Kjall, J. Isaksson, M. Sandberg, E. W. H. Jager, A. Richter-Dahlfors and M. Berggren, Adv. Mater., 2009, 21, 4442 CrossRef CAS PubMed  .

43. K. C. Larsson, P. Kjall and A. Richter-Dahlfors, Biochim. Biophys. Acta, 2013, 1830, 4334 CrossRef CAS PubMed.
44. S. Carrara, S. Ghoreishizadeh, J. Olivo, I. Taurino, C. Baj-Rossi, A. Cavallini, M. Op de Beeck, C. Dehollain, W. Burleson, F. G. Moussy, A. Guiseppi-Elie and G. De Micheli, Sensors, 2012, 12, 11013 CrossRef CAS PubMed.
45. G. Chan and D. J. Mooney, Trends Biotechnol., 2008, 26, 382 CrossRef CAS PubMed.
46. A. Guiseppi-Elie, Biomaterials, 2010, 31, 2701 CrossRef CAS PubMed.
47. C. Immerstrand, K. Holmgren-Peterson, K. E. Magnusson, E. Jager, M. Krogh, M. Skoglund, A. Selbing and O. Inganas, MRS Bull., 2002, 27, 461 CrossRef CAS Search PubMed.
48. S. C. Luo, Polym. Rev., 2013, 53, 303 CrossRef CAS Search PubMed.

49. H. von Holst, Biochim. Biophys. Acta, 2013, 1830, 4345 CrossRef CAS PubMed  .
50. Z. L. Yue, S. E. Moulton, M. Cook, S. O'Leary and G. G. Wallace, Adv. Drug Delivery Rev., 2013, 65, 559 CrossRef CAS PubMed  .
51. L. Poole-Warren, N. Lovell, S. Baek and R. Green, Expert Rev. Med. Devices, 2010, 7, 35 CrossRef CAS PubMed  .
52. R. A. Green, S. Baek, L. A. Poole-Warren and P. J. Martens, Sci. Technol. Adv. Mater., 2010, 11, 014107 CrossRef Search PubMed 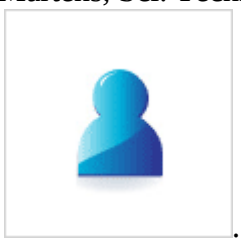 .
53. S. Baek, R. Green, A. Granville, P. Martens and L. Poole-Warren, J. Mater. Chem. B, 2013, 1, 3803 RSC  .
54. M. Muskovich and C. J. Bettinger, Adv. Healthcare Mater., 2012, 1, 248 CrossRef CAS PubMed  .

55. D. Svirskis, J. Travas-Sejdic, A. Rodgers and S. Garg, J. Controlled Release, 2010, 146, 6 CrossRef CAS PubMed  .
56. M. Berggren and A. Richter-Dahlfors, Adv. Mater., 2007, 19, 3201 CrossRef CAS PubMed  .
57. J. Rivnay, R. M. Owens and G. G. Malliaras, Chem. Mater., 2014, 26, 679 CrossRef CAS Search PubMed  .
58. V. Pillay, T. S. Tsai, Y. E. Choonara, L. C. du Toit, P. Kumar, G. Modi, D. Naidoo, L. K. Tomar, C. Tyagi and V. M. Ndesendo, J. Biomed. Mater. Res., Part B, 2014, 102, 2039 CrossRef PubMed  .
59. R. A. Green, N. H. Lovell, G. G. Wallace and L. A. Poole-Warren, Biomaterials, 2008, 29, 3393 CrossRef CAS PubMed  .
60. A. G. MacDiarmid, Angew. Chem., Int. Ed., 2001, 40, 2581 CrossRef CAS Search PubMed  .

61. X. F. Lu, W. J. Zhang, C. Wang, T. C. Wen and Y. Wei, Prog. Polym. Sci., 2011, 36, 671 CrossRef CAS PubMed  .
62. M. J. Higgins, P. J. Molino, Z. L. Yue and G. G. Wallace, Chem. Mater., 2012, 24, 828 CrossRef CAS Search PubMed  .
63. A. N. Zelikin, D. M. Lynn, J. Farhadi, I. Martin, V. Shastri and R. Langer, Angew. Chem., Int. Ed., 2002, 41, 141 CrossRef CAS Search PubMed  .
64. D. Mawad, P. J. Molino, S. Gambhir, J. M. Locke, D. L. Officer and G. G. Wallace, Adv. Funct. Mater., 2012, 22, 5020 CrossRef CAS PubMed  .
65. D. Mawad, E. Stewart, D. L. Officer, T. Romeo, P. Wagner, K. Wagner and G. G. Wallace, Adv. Funct. Mater., 2012, 22, 2692 CrossRef CAS PubMed  .
66. D. Mawad, K. Gilmore, P. Molino, K. Wagner, P. Wagner, D. L. Officer and G. G. Wallace, J. Mater. Chem., 2011, 21, 5555 RSC  .

67. L. Viry, S. E. Moulton, T. Romeo, C. Suhr, D. Mawad, M. Cook and G. G. Wallace, J. Mater. Chem., 2012, 22, 11347 RSC  .
68. Y. L. Hong and L. L. Miller, Chem. Mater., 1995, 7, 1999 CrossRef CAS Search PubMed  .
69. A. Mishra, C. Q. Ma and P. Bauerle, Chem. Rev., 2009, 109, 1141 CrossRef CAS PubMed  .
70. T. J. Rivers, T. W. Hudson and C. E. Schmidt, Adv. Funct. Mater., 2002, 12, 33 CrossRef CAS Search PubMed 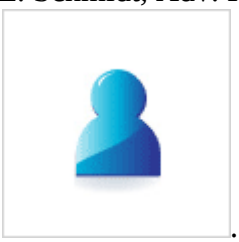 .
71. N. K. E. Guimard, J. L. Sessler and C. E. Schmidt, Macromolecules, 2009, 42, 502 CrossRef CAS PubMed  .
72. B. L. Guo, Y. Sun, A. Finne-Wistrand, K. Mustafa and A. C. Albertsson, Acta Biomater., 2012, 8, 144 CrossRef CAS PubMed  .

73. B. Guo, A. Finne-Wistrand and A. C. Albertsson, Biomacromolecules, 2011, 12, 2601 CrossRef CAS PubMed  .
74. B. L. Guo, A. Finne-Wistrand and A. C. Albertsson, Biomacromolecules, 2010, 11, 855 CrossRef CAS PubMed  .
75. B. Guo, A. Finne-Wistrand and A. C. Albertsson, Chem. Mater., 2011, 23, 4045 CrossRef CAS Search PubMed  .
76. B. L. Guo, A. Finne-Wistrand and A. C. Albertsson, Chem. Mater., 2011, 23, 1254 CrossRef CAS Search PubMed  .
77. B. L. Guo, A. Finne-Wistrand and A. C. Albertsson, J. Polym. Sci., Part A: Polym. Chem., 2011, 49, 2097 CrossRef CAS PubMed 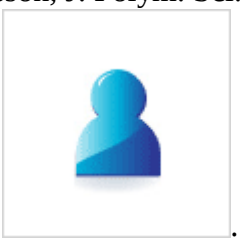 .
78. B. L. Guo, A. Finne-Wistrand and A. C. Albertsson, Macromolecules, 2010, 43, 4472 CrossRef CAS Search PubMed  .

79. B. L. Guo, A. Finne-Wistrand and A. C. Albertsson, Macromolecules, 2011, 44, 5227 CrossRef CAS Search PubMed  .
80. B. L. Guo, A. Finne-Wistrand and A. C. Albertsson, Macromolecules, 2012, 45, 652 CrossRef CAS Search PubMed  .
81. L. H. Huang, J. Hu, L. Lang, X. Wang, P. B. Zhang, X. B. Jing, X. H. Wang, X. S. Chen, P. I. Lelkes, A. G. MacDiarmid and Y. Wei, Biomaterials, 2007, 28, 1741 CrossRef CAS PubMed  .
82. H. T. Wu, T. Yu, Q. S. Zhu, Z. X. Jiao, Y. Wei, P. B. Zhang and X. S. Chen, Chem. Res. Chin. Univ., 2011, 32, 1181 CAS Search PubMed  .
83. Y. D. Liu, J. Hu, X. L. Zhuang, P. B. A. Zhang, X. S. Chen, Y. Wei and X. H. Wang, Macromol. Biosci., 2011, 11, 806 CrossRef CAS PubMed  .
84. Y. Guo, M. Y. Li, A. Mylonakis, J. J. Han, A. G. MacDiarmid, X. S. Chen, P. I. Lelkes and Y. Wei, Biomacromolecules, 2007, 8, 3025 CrossRef CAS PubMed  .

85. H. T. Cui, Y. D. Liu, M. X. Deng, X. Pang, P. B. A. Zhang, X. H. Wang, X. S. Chen and Y. Wei, Biomacromolecules, 2012, 13, 2881 CrossRef CAS PubMed  .
86. H. X. Qi, M. Y. Liu, L. X. Xu, L. Feng, L. Tao, Y. Ji, X. Y. Zhang and Y. Wei, J. Toxicol. Res., 2013, 2, 427 RSC  .
87. X. Y. Zhang, H. X. Qi, S. Q. Wang, L. Feng, Y. Ji, L. Tao, S. X. Li and Y. Wei, J. Toxicol. Res., 2012, 1, 201 RSC  .
88. L. H. Huang, X. L. Zhuang, J. Hu, L. Lang, P. B. Zhang, Y. S. Wang, X. S. Chen, Y. Wei and X. B. Jing, Biomacromolecules, 2008, 9, 850 CrossRef CAS PubMed  .
89. B. Zinger and L. L. Miller, J. Am. Chem. Soc., 1984, 106, 6861 CrossRef CAS Search PubMed  .
90. M. Pyo and J. R. Reynolds, Chem. Mater., 1996, 8, 128–133 CrossRef CAS Search PubMed  .

91. M. R. Abidian, D. H. Kim and D. C. Martin, Adv. Mater., 2006, 18, 405 CrossRef CAS PubMed  .
92. R. Wadhwa, C. F. Lagenaur and X. T. Cui, J. Controlled Release, 2006, 110, 531 CrossRef CAS PubMed  .
93. S. Sirivisoot, R. Pareta and T. J. Webster, Nanotechnology, 2011, 22, 085101 CrossRef PubMed  .
94. C. Gautier, C. Cougnon, J. F. Pilard, N. Casse and B. Chenais, Anal. Chem., 2007, 79, 7920 CrossRef CAS PubMed  .
95. L. L. Miller and Q. X. Zhou, Macromolecules, 1987, 20, 1594 CrossRef CAS Search PubMed  .
96. Q. X. Zhou, L. L. Miller and J. R. Valentine, J. Electroanal. Chem., 1989, 261, 147 CrossRef CAS Search PubMed  .

97. P. M. George, D. A. LaVan, J. A. Burdick, C. Y. Chen, E. Liang and R. Langer, Adv. Mater., 2006, 18, 577 CrossRef CAS PubMed 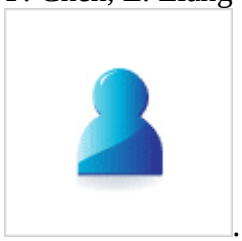 .
98. G. Bidan, C. Lopez, F. Mendesviegas, E. Vieil and A. Gadelle, Biosens. Bioelectron., 1995, 10, 219 CrossRef CAS Search PubMed  .
99. M. J. Knauf, D. P. Bell, P. Hirtzer, Z. P. Luo, J. D. Young and N. V. Katre, J. Biol. Chem., 1988, 263, 15064 CAS Search PubMed  .
100. F. Aucella, A. Gesuete, M. Vigilante and M. Prencipe, Blood Purif., 2013, 35, 42 CrossRef CAS PubMed  .
101. B. Chen, K. Jerger, J. M. J. Frechet and F. C. Szoka, J. Controlled Release, 2009, 140, 203 CrossRef CAS PubMed  .
102. L. Chen, Y. H. Yu, H. P. Mao, X. F. Lu, W. J. Zhang and Y. Wei, Chem. Res. Chin. Univ., 2004, 25, 1768 CAS Search PubMed  .

103. Q. Wang, Z. F. Dong, Y. M. Du and J. F. Kennedy, Carbohydr. Polym., 2007, 69, 336 CrossRef CAS PubMed  .
104. Y. Wang, H. D. Tran, L. Liao, X. F. Duan and R. B. Kaner, J. Am. Chem. Soc., 2010, 132, 10365 CrossRef CAS PubMed  .
105. Y. N. Xia, A. G. Macdiarmid and A. J. Epstein, Macromolecules, 1994, 27, 7212 CrossRef CAS Search PubMed  .
106. C. Gabriel, S. Gabriel and E. Corthout, Phys. Med. Biol., 1996, 41, 2231 CrossRef CAS Search PubMed  .
107. S. Gabriel, R. W. Lau and C. Gabriel, Phys. Med. Biol., 1996, 41, 2251 CrossRef CAS Search PubMed  .
108. S. Gabriel, R. W. Lau and C. Gabriel, Phys. Med. Biol., 1996, 41, 2271 CrossRef CAS Search PubMed  .

109. H. L. Lujan and S. E. DiCarlo, Med. Hypotheses, 2013, 81, 521 CrossRef CAS PubMed.
110. A. M. Altizer, L. J. Moriarty, S. M. Bell, C. M. Schreiner, W. J. Scott and R. B. Borgens, Dev. Dyn., 2001, 221, 391 CrossRef CAS PubMed.
111. H. Park, B. L. Larson, M. E. Kolewe, G. Vunjak-Novakovic and L. E. Freed, Exp. Cell Res., 2014, 321, 297 CrossRef CAS PubMed.
112. R. Saigal, E. Cimetta, N. Tandon, J. Zhou, R. Langer, M. Young, G. Vunjak-Novakovic and S. Redenti, Conf. Proc. IEEE Eng. Med. Biol. Soc., 2013, 2013, 1627 Search PubMed.
113. N. Tandon, E. Cimetta, A. Taubman, N. Kupferstein, U. Madaan, J. Mighty, S. Redenti and G. Vunjak-Novakovic, Conf. Proc. IEEE Eng. Med. Biol. Soc., 2013, 2013, 5666 Search PubMed.
114. W. L. Grayson, T. P. Martens, G. M. Eng, M. Radisic and G. Vunjak-Novakovic, Semin. Cell Dev. Biol., 2009, 20, 665 CrossRef CAS PubMed.

115. M. L. Kringelbach, A. L. Green, S. L. F. Owen, P. M. Schweder and T. Z. Aziz, Eur. J. Neurosci., 2010, 32, 1070 CrossRef PubMed  .
116. M. L. Kringelbach, N. Jenkinson, S. L. F. Owen and T. Z. Aziz, Nat. Rev. Neurosci., 2007, 8, 623 CrossRef CAS PubMed  .
117. M. A. da Silva, A. Crawford, J. Mundy, A. Martins, J. V. Araujo, P. V. Hatton, R. L. Reis and N. M. Neves, Tissue Eng., Part A, 2009, 15, 377 CrossRef PubMed 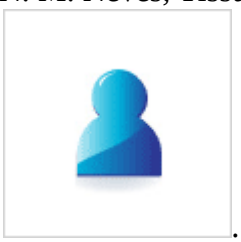 .
118. H. Jukola, L. Nikkola, M. E. Gomes, F. Chiellini, M. Tukiainen, M. Kellomaki, E. Chiellini, R. L. Reis and N. Ashammakhi, J. Biomed. Mater. Res., Part B, 2008, 87B, 197 CrossRef CAS PubMed  .
119. R. Webster, E. Didier, P. Harris, N. Siegel, J. Stadler, L. Tilbury and D. Smith, Drug Metab. Dispos., 2007, 35, 9 CrossRef CAS PubMed  .
120. H. F. Sun, L. Mei, C. X. Song, X. M. Cui and P. Y. Wang, Biomaterials, 2006, 27, 1735 CrossRef CAS PubMed  .

121. J. Hu, L. H. Huang, X. L. Zhuang, P. B. Zhang, L. Lang, X. S. Chen, Y. Wei and X. B. Jing, Biomacromolecules, 2008, 9, 2637 CrossRef CAS PubMed  .
122. Y. Liu, J. Hu, X. Zhuang, P. Zhang, X. Chen, Y. Wei and X. Wang, Macromol. Biosci., 2011, 11, 806 CrossRef CAS PubMed  .
123. Q. S. Zhang, Y. H. Yan, S. P. Li and T. Feng, Mater. Sci. Eng., C, 2010, 30, 160 CrossRef CAS PubMed  .
124. Q. S. Zhang, Y. H. Yan, S. P. Li and T. Feng, Biomed. Mater., 2009, 4 Search PubMed  .
125. C. M. Boutry, H. Chandrahalim, P. Streit, M. Schinhammer, A. C. Hanzi and C. Hierold, Philos. Trans. R. Soc., A, 2012, 370, 2418 CrossRef CAS PubMed 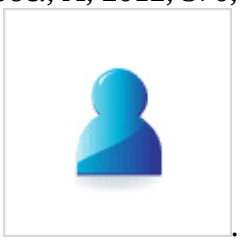 .
126. B. B. Yue, C. Y. Wang, P. Wagner, Y. Yang, X. Ding, D. L. Officer and G. G. Wallace, Synth. Met., 2012, 162, 2216 CrossRef CAS PubMed  .

127. S. Li, Z. P. Guo, C. Y. Wang, G. G. Wallace and H. K. Liu, J. Mater. Chem. A, 2013, 1, 14300 CAS Search PubMed.
128. D. Persaud-Sharma and A. McGoron, J. Biomimetics, Biomater., Tissue Eng., 2012, 12, 25 CrossRef PubMed.
129. Y. J. Kim, S. E. Chun, J. Whitacre and C. J. Bettinger, J. Mater. Chem. B, 2013, 1, 3781 RSC.
130. A. Walcarius, S. D. Minteer, J. Wang, Y. H. Lin and A. Merkoci, J. Mater. Chem. B, 2013, 1, 4878 RSC.
131. M. J. Moehlenbrock and S. D. Minteer, Chem. Soc. Rev., 2008, 37, 1188 RSC.
132. C. J. Bettinger and Z. A. Bao, Polym. Int., 2010, 59, 563 CAS Search PubMed.

133. R. L. Arechederra and S. D. Minteer, Anal. Bioanal. Chem., 2011, 400, 1605 CrossRef CAS PubMed 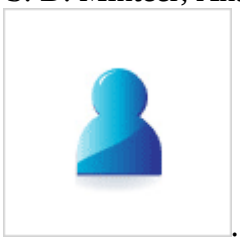 .
134. W. B. Liechty and N. A. Peppas, Eur. J. Pharm. Biopharm., 2012, 80, 241 CrossRef CAS PubMed  .
135. S. Brahim, D. Narinesingh and A. Guiseppi-Elie, Biosens. Bioelectron., 2002, 17, 973 CrossRef CAS Search PubMed  .
136. D. M. Thompson, A. N. Koppes, J. G. Hardy and C. E. Schmidt, Annu. Rev. Biomed. Eng., 2014, 16, 397 CrossRef CAS PubMed  .
137. J. G. Hardy, A. Leal-Egaña and T. R. Scheibel, Macromol. Biosci., 2013, 13, 1431 CrossRef CAS PubMed  .
138. J. G. Hardy, A. Pfaff, A. Leal-Egaña, A. H. E. Müller and T. R. Scheibel, Macromol. Biosci., 2014, 14, 936 CrossRef CAS PubMed  .